LncRNA LINC00337 Sponges miR-1285-3p to Promote Proliferation and Metastasis of Lung Adenocarcinoma Cells Through Up-Regulating YTHDF1

Ru-nan Zhang (wdjzz95@163.com)
Xinxiang Central Hospital https://orcid.org/0000-0002-5458-406X
Dong-mei Wu
Xinxiang Central Hospital
Li-ping Wu
Xinxiang Central Hospital
Guo-wei Gao
Xinxiang Central Hospital

Primary research

Keywords: lung adenocarcinoma, lncRNA, LINC00337, cell invasion, cell proliferation

Posted Date: August 11th, 2020

DOI: https://doi.org/10.21203/rs.3.rs-56092/v1

Abstract

Background: Emerging studies have attested that long noncoding RNAs (lncRNAs) predominantly functioned in carcinogenesis of multiple developing human tumors. The current research aimed at probing the underlying participation and mechanisms of *LINC00337* in lung adenocarcinoma.

Methods: Here we analyzed TCGA and GTEx datasets and chose *LINC00337* as research object. Cell proliferation, cell apoptosis, cell cycle, and invasion were detected in gain and loss experiment of *LINC00337* both *in vitro* and *in vivo*. Moreover, RNA pull-down, luciferase reporter assays, western blotting analysis, rescue experiment were performed to investigate underlying molecular mechanisms of *LINC00337* function.

Results: *LINC00337* was remarkably increased in lung adenocarcinoma. Also, *LINC00337* knock-down was unraveled to repress cell invasion and proliferation as well as cell cycle, and gear up apoptosis in lung adenocarcinoma *in vitro* and *in vivo*. With respect to mechanism, *LINC00337* knock-down boosted miR-1285-3p to be expressed and then restrained *YTHDF1* to be expressed post-transcriptionally. Crucially, both miR-1285-3p decrement and *YTHDF1* overexpression successfully countered the influence on cell proliferation, invasion and apoptosis caused by *LINC00337* shRNA.

Conclusions: These results suggest that *LINC00337* acted as an oncogenic lncRNA, targeting miR-1285-3p and regulating *YTHDF1* expression, to promote the progression of lung adenocarcinoma.

Background

As a frequently seen malignant tumor, lung cancer turns out to be the chief cause of global cancer-involved death[1, 2]. Lung cancer is histologically assorted into large cell carcinoma, squamous cell carcinoma, adenocarcinoma and bronchoalveolar carcinoma[3]. Lung cancer patients have low overall five-year survival rate (about 18.1%). Lung adenocarcinoma cases take up near 40% of lung cancer ones[4, 5]. Therefore, it is of great significance to look for novel biomarkers and targets for early diagnosing and treating lung cancer.

Human genomic sequencing uncovers the active transcription of exceeding ninety percent of genomes, among which two percent is the RNA that encodes proteins and the remaining is the RNA unable to encode proteins[6, 7]. Long noncoding RNA (LncRNA) are ncRNAs longer than 200 nt[8, 9], and quite a few lncRNAs are expressed with specificity to cell types[10-12] and possess exact positions of subcellular compartments[13-15]. Additionally, expression of numerous lncRNAs has been demonstrated to interrelate to the progression of diverse cancers, which are able to modulate cancer cell proliferation and apoptosis.[16-19] According to reports, *LINC00337* is a pro-tumor factor in gastric cancer[20] and esophageal cancer[21], but its function in lung adenocarcinoma remains elusive.

In current research, we analyzed the TCGA and GTEx datasets, and *LINC00337* was dramatically higher in lung adenocarcinoma tissues relative to para-tumor ones. In TCGA dataset, high *LINC00337* level

indicated shorter overall survival. We also examined samples surgically resected from 46 lung adenocarcinoma cases at our institution to figure out differences in expression level of *LINC00337* between lung adenocarcinoma tissues and normal ones, and the result was in consistency with the analyses of TCGA and GTEx datasets. Then, we conducted a series of experiments to explore whether *LINC00337* participated in the onset and development process of lung adenocarcinoma and the mechanism of its function.

Materials And Methods

Collection of clinical samples

From 2017 to 2019, 46 paired fresh lung adenocarcinoma and para-tumor tissues were harvested in our hospital. We snap-freezed these tissues at -80°C. Patients received no preoperative chemotherapy or radiotherapy. All included subjects offered an informed consent and the research got approval from the Institutional Review Board of Xinxiang Central Hospital. Thorough clinical and pathological features of patients with lung adenocarcinoma are summed up in Table 1.

Table 1. The correlation of LINC00337 expression with clinical parameters in patients with lung adenocarcinoma

Clinicopathological features	Number of cases	LINC00337 expression		*p* value
		High (n=23)	Low (n=23)	
Gender				0.2362
Male	25	10	15	
Female	21	13	8	
Age				0.7683
<60	24	13	11	
≥60	22	10	12	
Tumor size				0.0377*
≤5	24	8	16	
□5	22	15	7	
TNM stages				0.0058*
□/□□	28	9	19	
□/□	18	14	4	
Lymph node metastasis				0.0072*
Absent	24	17	7	
Present	22	6	16	

Total data from 46 lung adenocarcinoma patients were analyzed. For the expression of LINC00337 was assayed by qRT-PCR, the median expression level was used as the cutoff. Data were analyzed by chi-squared test. P-value in bold indicates statistically significant.

Cell culture

Lung adenocarcinoma cell lines (PC-9, H1373, HCC827 and A549) and normal human lung epithelial cell line (BEAS2B) were collected from Cell Resource of CAMS (Beijing, China), cultured in RPMI-1640 medium with 10% FBS (Gibco, CA) and preserved at 37°C with 5% CO_2.

shRNAs and anti-miRNA inhibitors

Genechem (Shanghai, China) synthetized shRNAs targeting *LINC00337* (shRNA#1, 2) and *YTHDF1* (sh-*YTHDF1*) and negative control shRNA (sh-NC) without exact target. RiboBio (Guangzhou, China) provided inhibitors against miR-1285-3p (anti-miR-1285-3p) and miR-NC (anti-miR-NC). Subsequent to seeding of PC-9 or A549 cells in six-well plates for twenty-four hours, they received transfection with Lipofectamine 2000 offered by Invitrogen (Shanghai, China) in the case of 40-60% confluence *as per* manufacturer's guidance. Forty-eight hours later, cells were collected, and stable cells were chosen for four-week therapy with neomycin (500 μg/mL).

RNA isolation andquantitative real-time PCR (qRT-PCR)

As per the manufacturer's guidance, total RNA segregation was implemented using TRIzol from Invitrogen, and it was then synthesized into cDNA using stochastic primers *via* a PrimeScript RT reagent Kit from Takara (Dalian, China) or a miRNA reverse transcription PCR kit commercially offered by RiboBio. QRT-PCR analysis was implemented using the SYBR Premix Ex Taq kit from Takara. The utilized primers are listed below: *LNC00337*: 5'-CCAGACTGGAGAACCACAGC-3' (forward) and 5' CTGTGTCTATGTGCAGCCCT-3' (reverse), miR-1285-3p: 5'- TCTGGGCAACAAAGTGAG-3' (forward) and 5'-CTCAACTGGTGTCGTGGA-3' (reverse), *YTHDF1*: 5'-ACCTGTCCAGCTATTACCCG-3' (forward) and 5'-TGGTGAGGTATGGAATCGGAG-3' (reverse). Bulge-Loop miRNAs qPCR Primers were offered by RiboBio, and data were processed *via* StepOnePlus Real-Time PCR System offered by Applied Biosystems (Shanghai, China), whose results were evaluated with GAPDH or U6 expression as standard.

Western blot evaluation

RIPA extraction liquid from Beyotime (Jiangsu, China) in the presence of Protease Inhibitor Cocktail and PMSF (Roche, Shanghai, China) was utilized for lysis of assembled cells. Subsequent to examination of protein sample concentration *via* BCA Protein Assay Kit from Beyotime, the harvested proteins in commensurable amounts were set apart by SDS-PAGE (10% gel) and transferred to PVDF membranes, which underwent 1-h sealing by Tris-buffered saline (5% defatted milk) and 12-h primary antibody incubation at 4°C. Next, optical density method was adopted to quantitate autoradiographs using Quantity One software (Bio-Rad) with GAPDH (#2118; CST, Shanghai, China) as a reference. Anti-*YTHDF1* (#86463), anti-E-cadherin (#3195), anti-Vimentin (#5741) antibodies were provided by CST.

Immunohistochemistry

Nude mouse tumor tissues implanted by paraffin received immunostaining, and expression level and position of target proteins were ascertained using avidin-biotin-peroxidase method. Next, primary antibodies against E-cadherin and Vimentin were diluted at 1:200 for later application. Tumor apoptosis and proliferation were appraised by independently probing Ki-67 and Bax. Lastly, slice visualization was achieved using a microscope from Olympus (Japan).

5-ethynyl-20-deoxyuridine assay (EdU) Assay

Cell proliferation was also proved by Ethynyl-2-deoxyuridine incorporation assay using an EdU Apollo DNA *in vitro* kit (RIBOBIO, Guangzhou, China) *as per* the manufacturer's guidance. Briefly, subsequent to transfection with the corresponding vector, cells received respective 2-h incubation at 37 °C, with 100 μl of 50 μM EdU/well. *Via* a fluorescence microscopy, the cells were identified. We carried out each experiment for three times.

Cell Counting Kit-8 assay

Cell Counting Kit-8 (Beyotime Inst Biotech, China) was used to determine cell proliferation. In a word, 5×10^3 cells/well underwent 1-day raising in a 96-well broad-bottomed plate at 37°C, followed by transfecting them with corresponding vectors. Finally, with a microplate reader from Bio-Rad (Shanghai, China), the absorbance was finally evaluated at 450 nm, and we carried out each experiment for three times.

Apoptosis and cell cycle experiments

As per the manufacturer's guidance, apoptosis determination was implemented *via* FACS using PE-Annexin V apoptosis detection kit from BD Pharmingen (Shanghai, China) subsequent to 48-h transfection, and cell cycle was assessed utilizing PI cell cycle assessment kits (BD Pharmingen). Each assay was implemented thrice.

Transwell assay

Transwell chambers were used to observe the invasion of lung adenocarcinoma cells. We seeded cancer cells in the upper chamber coated by Matrigel (Corning, USA, dilution ratio: 1:6) at a density of 10^5 cells per well and supplemented DMEM with 1% FBS. Later we filled 600μL DMEM with 10% FBS into the lower chamber, fixed cells by 4% methanol and stained them with crystal violet. Then we counted them in 5 random 200× microscopic fields, after cells being invaded to the lower surface of membrane and incubated at 37°C for 24 hours. We carried out each experiment for three times.

Dual-Luciferase Reporter Assay

Genechem designed and synthesized *YTHDF1* full-length promoter reporter vector. Human *YTHDF1* 3'-untranslated region (UTR) fragment with supposed binding sites for miR-1285-3p reporter vector was offered by RiboBio. 48-h transfection later, Dual-Luciferase Reporter Assay System from Promega was adopted for luciferase activity determination *as per* the manufacturer's guidance, and luciferase activity ratio (Firefly/Renilla) was ascertained. Each assay was implemented thrice.

RNA pull-down assay

The DNA fragment with the full length *LINC00337* or NC sequence received PCR amplification using a primer with T7 and was cloned into GV394 from Genechem, Shanghai, China). Restriction enzyme XhoI was utilized for linearization of DNAs. Next, T7 RNA polymerase (Takara) and Biotin RNA Labeling Mix

from Roche (China) were employed for reverse transcription of biotin-labeled RNAs underwent reverse transcription. Thereafter, the products received DNase I (RNase-free, Roche) treatment and purification using the RNeasy Mini Kit (Qiagen, USA), and the extracted RNAs were employed for qRT-PCR assessment.

Tumor xenograft implantation in nude mice

We divided six-week-old nude mice into two groups (4 mice/group) randomly, raised them with unceasing food and water in sterile conditions without pathogens. To establish the lung adenocarcinoma xenograft model, we subcutaneously injected A549 cells into nude mice. We monitored tumor growth every week and calculated it as equation: Volume = (Length) × $(Width)^2/2$. Animal assays took place in SPF Animal Laboratory at Xinxiang Medical University, and experiments were performed following the NIH guidelines on animal welfare.

Statistical analysis

Differences of data in normal distribution and equal variance were processed by 2-tailed Student t test (2-group comparisons) or ANOVA, and the post hoc Bonferroni test (multigroup comparisons) was implemented as appropriate. Differences of data in non-normal distribution or unequal variance were processed by a nonparametric Mann-Whitney U test (2-group comparisons) or the Kruskal-Wallis test followed by the post hoc Bonferroni test (multigroup comparisons). The standard we used to determine statistical significance was that $P<0.05$. We carried out all tests via SPSS 22.0 (SPSS, Chicago, IL, USA).

Results

LINC00337 is elevated in lung adenocarcinoma tissues and cells and dramatically present in the cell cytoplasm

Through the analysis of TCGA and GTEx database, we unraveled that *LINC00337* was dramatically raised in lung adenocarcinoma tissues (from TCGA database) relative to normal tissues (from GTEx database) (Fig. 1A, B). We then verified in 46 lung adenocarcinoma tissues and adjacent nontumorous tissues by qRT-PCR assays, and the result was consistent with previous analyses of TCGA and GTEx database (Fig. 1C). Similarly, higher *LINC00337* levels were showed in lung adenocarcinoma cells (PC-9, H1373, HCC827 and A549) rather than normal human lung epithelial cell line BEAS2B (Fig. 1D). Additionally, PC-9 and A549 cells were picked up for later assays. In addition, *LINC00337* expression levels in lung adenocarcinoma evidently interrelated to high-grade cancer, lymph node metastasis and tumor size instead of other parameters such as age or gander (Table 1). TCGA database showed that the overall survival rate of patients with low *LINC00337* level was higher relative to that of patients with high *LINC00337* level (Fig. 1E). Then, we examined the subcellular localization of *LINC00337* and found that most of *LINC00337* was present in the cell cytoplasm in lung adenocarcinoma cells (Fig. 1F).

Knockdown of *LINC00337* curbs cell cycle, proliferation and invasion but boosts apoptosis of lung adenocarcinoma cells

To determine whether *LINC00337* functions in lung adenocarcinoma cells, we implemented a variety of *in vitro* assays to assess the impact of shRNA knockdown of *LINC00337* and overexpression of *LINC00337* on cell functions including proliferation, apoptosis, and invasion. PC-9 transfected with *LINC00337* overexpression vector and A549 cells transfected with sh-*LINC00337* (Fig. 2A). CCK-8 and EdU assays showed that overexpression of *LINC00337* promoted proliferation of PC-9 cells, sh-*LINC00337* attenuated proliferation of A549 cells (Fig. 2B, C). *LINC00337* knockdown reduced cell cycle arrest at S phase in A549 cells compared with negative control, and overexpression of *LINC00337* brought on cell cycle arrest at S phase in PC-9 cells (Fig. 2D). In Fig. 2E, evidently elevated apoptotic cell ratio was observed in sh-*LINC00337* group relative to sh-NC cells, and brought down apoptotic cell proportion in *LINC00337*-transfected cells relative to vector-transfected cells. Meanwhile, the invasion of cells was considerably elevated by overexpression of *LINC00337*, and decreased by sh-*LINC00337* (Fig. 2F). All above-mentioned data ascertained that knockdown of *LINC00337* curbs cell cycle, proliferation and invasion, and boosts apoptosis of lung adenocarcinoma cells.

LINC00337 interplayed with miR-1285-3p in a direct manner

LncRNA is a new-found regulatory mechanism affecting post-transcriptional control, disturbing miRNA pathways and acting like a natural miRNA sponge to reduce binding of endogenous miRNAs to target genes[22-25]. Through searching in online bioinformatics database (RegRNA 2.0, http://regrna2.mbc.nctu.edu.tw/), we observed that 6 miRNAs (hsa-miR-492, hsa-miR-1285-3p, hsa-miR-1304-5p, hsa-miR-1273a, hsa-miR-5095, hsa-miR-1273g-3p) possessed supposed binding sites with *LINC00337* (Fig. 3A).

Later, we utilized the pull-down system labeled by biotin to continuously probe miRNAs interplaying with *LINC00337* in a direct way. We unraveled an enormous body of miR-1285-3p in the *LINC00337* pull-down pellet relative to control group as examined by qRT-PCR, but the proportions of miR-492, miR-1273a, miR-5095, miR-1273g-3p, and miR-1304-5p in the *LINC00337* pull-down pellet displayed unobvious elevation relative to control group (Fig. 3B, C). Moreover, miR-1285-3p was expressed in lung adenocarcinoma samples at a declined level relative to normal samples (Fig. 3D). And overexpression of *LINC00337* decreased miR-1285-3p expression level tested by qRT-PCR (Fig. 3E). All above-mentioned data ascertained that *LINC00337* could sponge miR-1285-3p directly and specifically.

LINC00337 regulates the miR-1285-3p target gene, *YTHDF1*

Through searching in miRDB, we observed that 7 target genes of miR-1285-3p which score >95: AHI1, DAB2IP, BTRC, *YTHDF1*, TMEM41B, SIKE1, and FMO5. After reviewing the literature, we disclosed that only *YTHDF1* was bound up with lung adenocarcinoma[26-28]. As such, we surmised that *LINC00337* functioned via influencing *YTHDF1* expression in lung adenocarcinoma. We showed the binding sites of *YTHDF1* and miR-1285-3p in Fig. 4A. Result of qRT-PCR showed that *YTHDF1* level in cancer tissues was

significantly increased (Fig. 4B), and western blot showed down-regulation of *LINC00337* decreased the protein level of *YTHDF1* (Fig. 4C).

Afterwards, Dual-luciferase Reporter Assays were implemented using human *YTHDF1* 3'-UTR fragment with supposed binding sites of miR-1285-3p and *YTHDF1* promoter reporter vector for notarizing impact of miR-1285-3p on *YTHDF1*. It was unveiled that cells with stable sh-*LINC00337* transfection exhibited dramatically declined relative luciferase activity of *YTHDF1*-3'-UTR (Fig. 4D). And overexpression of *LINC00337* increased the luciferase activity in cells with stable *LINC00337* overexpression vector transfection (Fig. 4D). However, transfection of sh-*LINC00337* or *LINC00337* overexpression vector did not change promoter activity of *YTHDF1* in PC-9 and A549 cells (Fig. 4E). Further, decrement of miR-1285-3p with anti-miR-1285-3p successfully hindered the decrement of *YTHDF1* protein level induced by *LINC00337* shRNA (Fig. 4F). It could be inferred that *LINC00337* controlled *YTHDF1* expression at miR-1285-3p-adjusted posttranscriptional level. Transfection efficiency of miR-1285-3p mimics and anti-miR-1285-3p were shown in Additional file 1: Fig. S1A.

LINC00337/miR-1285-3p / *YTHDF1* axis regulates behaviors of lung adenocarcinoma cells

Subsequently, we explored the effect of *LINC00337*/ miR-1285-3p / *YTHDF1* axis on lung adenocarcinoma. We transfected sh-*YTHDF1* in PC-9 cells and transfected *YTHDF1* overexpression vector in A549 cells (Additional file 1: Fig. S1B). From Fig. 5A, we found that both knockdown of miR-1285-3p and up-regulated of YTHDF1 reversed the cell proliferation reduced by LINC00337 shRNA. And both knockdown of YTHDF1 and up-regulated of miR-1285-3p reversed the cell proliferation induced by LINC00337 overexpression. Cell apoptosis and invasion assays showed the same trend, that both knock-down of *YTHDF1* and up-regulation of miR-1285-3p reversed the influence caused by overexpression of *LINC00337* on cell apoptosis and invasion (Fig. 5B, C). These data suggested that *LINC00337* modulated lung adenocarcinoma *in vitro* through miR-1285-3p / *YTHDF1* axis.

Inhibition of *LINC00337* suppresses lung adenocarcinoma tumor to grow and metastasize *in vivo*

For continuously ascertaining the capability of inhibiting anti-tumorigenesis potential of *LINC00337* inhibition *in vivo*, stable A549 cells transfected with sh-NC or sh-*LINC00337* were inoculated into nude mice. Mice in sh-*LINC00337* group had decreased tumor volume and weight after assay relative to sh-NC group (Fig. 6A-C). Further, *LINC00337* knock-down curbed tumor to proliferate and boosted cell apoptosis (Fig. 6D). Western blot assay, qRT-PCR, and histological research of excised tumor tissues implied positive interrelation of *LINC00337* expression with *YTHDF1* and Vimentin as well as inverse interrelation with miR-1285-3p and E-cadherin in *LINC00337* repression and control groups (Fig. 6E-H). Furthermore, HE staining of mouse lung slices unveiled that suppressing *LINC00337* cut down metastatic nodule number in the lung relative to NC group (Fig. 6I). Above-mentioned findings uncovered potential of *LINC00337* in tumor metastasis and proliferation and offered more support for treatment regimen targeting *LINC00337* in lung adenocarcinoma.

Discussion

In this research, we analyzed TCGA and GTEx dataset and chose *LINC00337* as research object, which was expressed at a notably higher level in lung adenocarcinoma tissues and paired para-tumor tissues. Besides, *LINC00337* knock-down significantly curbed lung adenocarcinoma cells to proliferate and invade and arrested cell cycle, but boosted apoptosis *in vitro* and *in vivo*.

Like proteins, the function of lncRNAs depends on their subcellular localization[29]. Cytoplasmic lncRNAs that mostly localize and function in the cytoplasm act as decoys for miRNAs and proteins to affect gene modulation[30, 31]. Several studies reveal that lncRNAs are sponges of many miRNAs, exerting the same function as ceRNAs in tumorigenesis[32, 33].

Through subcellular localization experiment, we found that most of *LINC00337* was present in the cytoplasm of lung adenocarcinoma cells, suggesting that *LINC00337* might function at posttranscriptional level. In this case, *LINC00337* may act as a ceRNA to disturb miRNA pathways and control the contra-suppression of miRNA targets. So, we predicted miRNA and its downstream targets which may be associated with *LINC00337via* searching in RegRNA 2.0, miRDB. RNA pull-down assay, dual-luciferase reporter assay, qRT-PCR, and western blot were implemented to prove the association. Results showed that *LINC00337* functions as miR-1285-3p sponge to control *YTHDF1* in a positive manner. Subsequent cell function tests confirmed that both knockdown of *YTHDF1* and up-regulated of miR-1285-3p reversed the influence caused by overexpression of *LINC00337* on cell invasion, proliferation and apoptosis.

Conclusion

In conclusion, we identified that *LINC00337* was upregulated in lung adenocarcinoma and correlated with poor survival outcome in lung adenocarcinoma patients. And *LINC00337* acted as an oncogenic lncRNA, targeting miR-1285-3p and regulating *YTHDF1* expression, to promote the progression of lung adenocarcinoma.

Declarations

Ethics statement

The present research gained approval from the Ethics Committee of Xinxiang Central Hospital and Written informed consent from patients was obtained. Animal experiments took place in SPF Animal Laboratory at Xinxiang Medical University. All animal assays were implemented *as per* the Guide for the Care and Use of Laboratory Animals by NIH.

Consent for publication

All authors involved in the study had given their consent for submitting this article for publication

Availability of data and materials

Datasets used and/or analyzed during this study are available from the corresponding author on reasonable request.

Competing interests

The authors declare that they have no conflict of interest.

Funding

This research did not receive any specific grant from funding agencies in the public, commercial, or not-for-profit sectors.

Authors' contributions

RZ designed and conducted the majority of the experiments and manuscript writing. DW assisted with the results collection and processing. LW and GG instructed data analysis and figure production.

Acknowledgements

Not applicable

References

1. Hao X, Han F, Ma B, Zhang N, Chen H, Jiang X, Yin L, Liu W, Ao L, Cao J *et al*: **SOX30 is a key regulator of desmosomal gene suppressing tumor growth and metastasis in lung adenocarcinoma**. *J Exp Clin Cancer Res* 2018, **37**(1):111.
2. Lee G, Park H, Sohn I, Lee SH, Song SH, Kim H, Lee KS, Shim YM, Lee HY: **Comprehensive Computed Tomography Radiomics Analysis of Lung Adenocarcinoma for Prognostication**. *Oncologist* 2018, **23**(7):806-813.
3. Sun Y, Zhao J, Yin X, Yuan X, Guo J, Bi J: **miR-297 acts as an oncogene by targeting GPC5 in lung adenocarcinoma**. *Cell Prolif* 2016, **49**(5):636-643.
4. Alam H, Li N, Dhar SS, Wu SJ, Lv J, Chen K, Flores ER, Baseler L, Lee MG: **HP1gamma Promotes Lung Adenocarcinoma by Downregulating the Transcription-Repressive Regulators NCOR2 and ZBTB7A**. *Cancer Res* 2018, **78**(14):3834-3848.
5. Hegab AE, Ozaki M, Kameyama N, Gao J, Kagawa S, Yasuda H, Soejima K, Yin Y, Guzy RD, Nakamura Y *et al*: **Effect of FGF/FGFR pathway blocking on lung adenocarcinoma and its cancer-associated fibroblasts**. *J Pathol* 2019, **249**(2):193-205.
6. Tichon A, Perry RB, Stojic L, Ulitsky I: **SAM68 is required for regulation of Pumilio by the NORAD long noncoding RNA**. *Genes Dev* 2018, **32**(1):70-78.

7. Zhang Y, Tao Y, Liao Q: **Long noncoding RNA: a crosslink in biological regulatory network**. *Brief Bioinform* 2018, **19**(5):930-945.
8. Shen SN, Li K, Liu Y, Yang CL, He CY, Wang HR: **Down-regulation of long noncoding RNA PVT1 inhibits esophageal carcinoma cell migration and invasion and promotes cell apoptosis via microRNA-145-mediated inhibition of FSCN1**. *Mol Oncol* 2019, **13**(12):2554-2573.
9. Lian Y, Xiong F, Yang L, Bo H, Gong Z, Wang Y, Wei F, Tang Y, Li X, Liao Q *et al*: **Long noncoding RNA AFAP1-AS1 acts as a competing endogenous RNA of miR-423-5p to facilitate nasopharyngeal carcinoma metastasis through regulating the Rho/Rac pathway**. *J Exp Clin Cancer Res* 2018, **37**(1):253.
10. Hu W, Wang T, Yang Y, Zheng S: **Tumor heterogeneity uncovered by dynamic expression of long noncoding RNA at single-cell resolution**. *Cancer Genet* 2015, **208**(12):581-586.
11. Baskozos G, Dawes JM, Austin JS, Antunes-Martins A, McDermott L, Clark AJ, Trendafilova T, Lees JG, McMahon SB, Mogil JS *et al*: **Comprehensive analysis of long noncoding RNA expression in dorsal root ganglion reveals cell-type specificity and dysregulation after nerve injury**. *Pain* 2019, **160**(2):463-485.
12. Reddy AS, O'Brien D, Pisat N, Weichselbaum CT, Sakers K, Lisci M, Dalal JS, Dougherty JD: **A Comprehensive Analysis of Cell Type-Specific Nuclear RNA From Neurons and Glia of the Brain**. *Biol Psychiatry* 2017, **81**(3):252-264.
13. Chen LL: **Linking Long Noncoding RNA Localization and Function**. *Trends Biochem Sci* 2016, **41**(9):761-772.
14. Guo J, Liu Z, Gong R: **Long noncoding RNA: an emerging player in diabetes and diabetic kidney disease**. *Clin Sci (Lond)* 2019, **133**(12):1321-1339.
15. Chen S, Chen JZ, Zhang JQ, Chen HX, Qiu FN, Yan ML, Tian YF, Peng CH, Shen BY, Chen YL *et al*: **Silencing of long noncoding RNA LINC00958 prevents tumor initiation of pancreatic cancer by acting as a sponge of microRNA-330-5p to down-regulate PAX8**. *Cancer Lett* 2019, **446**:49-61.
16. Shang AQ, Wang WW, Yang YB, Gu CZ, Ji P, Chen C, Zeng BJ, Wu JL, Lu WY, Sun ZJ *et al*: **Knockdown of long noncoding RNA PVT1 suppresses cell proliferation and invasion of colorectal cancer via upregulation of microRNA-214-3p**. *Am J Physiol Gastrointest Liver Physiol* 2019, **317**(2):G222-G232.
17. Song F, Li L, Liang D, Zhuo Y, Wang X, Dai H: **Knockdown of long noncoding RNA urothelial carcinoma associated 1 inhibits colorectal cancer cell proliferation and promotes apoptosis via modulating autophagy**. *J Cell Physiol* 2019, **234**(5):7420-7434.
18. Zhao Y, Zhao L, Li J, Zhong L: **Silencing of long noncoding RNA RP11-476D10.1 enhances apoptosis and autophagy while inhibiting proliferation of papillary thyroid carcinoma cells via microRNA-138-5p-dependent inhibition of LRRK2**. *J Cell Physiol* 2019, **234**(11):20980-20991.
19. Liu S, Yan G, Zhang J, Yu L: **Knockdown of Long Noncoding RNA (lncRNA) Metastasis-Associated Lung Adenocarcinoma Transcript 1 (MALAT1) Inhibits Proliferation, Migration, and Invasion and Promotes Apoptosis by Targeting miR-124 in Retinoblastoma**. *Oncol Res* 2018, **26**(4):581-591.

20. Hu B, Wang X, Li L: **Long noncoding RNA LINC00337 promote gastric cancer proliferation through repressing p21 mediated by EZH2**. *Am J Transl Res* 2019, **11**(5):3238-3245.
21. Yang C, Shen S, Zheng X, Ye K, Ge H, Sun Y, Lu Y: **Long non-coding RNA LINC00337 induces autophagy and chemoresistance to cisplatin in esophageal squamous cell carcinoma cells via upregulation of TPX2 by recruiting E2F4**. *FASEB J* 2020, **34**(5):6055-6069.
22. Yoon JH, Abdelmohsen K, Gorospe M: **Posttranscriptional gene regulation by long noncoding RNA**. *J Mol Biol* 2013, **425**(19):3723-3730.
23. Hammerle M, Gutschner T, Uckelmann H, Ozgur S, Fiskin E, Gross M, Skawran B, Geffers R, Longerich T, Breuhahn K *et al*: **Posttranscriptional destabilization of the liver-specific long noncoding RNA HULC by the IGF2 mRNA-binding protein 1 (IGF2BP1)**. *Hepatology* 2013, **58**(5):1703-1712.
24. Li C, Gao Q, Wang M, Xin H: **LncRNA SNHG1 contributes to the regulation of acute myeloid leukemia cell growth by modulating miR-489-3p/SOX12/Wnt/beta-catenin signaling**. *J Cell Physiol* 2020.
25. Podralska M, Ciesielska S, Kluiver J, van den Berg A, Dzikiewicz-Krawczyk A, Slezak-Prochazka I: **Non-Coding RNAs in Cancer Radiosensitivity: MicroRNAs and lncRNAs as Regulators of Radiation-Induced Signaling Pathways**. *Cancers (Basel)* 2020, **12**(6).
26. Li X, Li N, Huang L, Xu S, Zheng X, Hamsath A, Zhang M, Dai L, Zhang H, Wong JJ *et al*: **Is Hydrogen Sulfide a Concern During Treatment of Lung Adenocarcinoma With Ammonium Tetrathiomolybdate?** *Front Oncol* 2020, **10**:234.
27. Zhuang Z, Chen L, Mao Y, Zheng Q, Li H, Huang Y, Hu Z, Jin Y: **Diagnostic, progressive and prognostic performance of m(6)A methylation RNA regulators in lung adenocarcinoma**. *Int J Biol Sci* 2020, **16**(11):1785-1797.
28. Shi Y, Fan S, Wu M, Zuo Z, Li X, Jiang L, Shen Q, Xu P, Zeng L, Zhou Y *et al*: **YTHDF1 links hypoxia adaptation and non-small cell lung cancer progression**. *Nat Commun* 2019, **10**(1):4892.
29. Mas-Ponte D, Carlevaro-Fita J, Palumbo E, Hermoso Pulido T, Guigo R, Johnson R: **LncATLAS database for subcellular localization of long noncoding RNAs**. *RNA* 2017, **23**(7):1080-1087.
30. Yang R, Xing L, Wang M, Chi H, Zhang L, Chen J: **Comprehensive Analysis of Differentially Expressed Profiles of lncRNAs/mRNAs and miRNAs with Associated ceRNA Networks in Triple-Negative Breast Cancer**. *Cell Physiol Biochem* 2018, **50**(2):473-488.
31. Tran DDH, Kessler C, Niehus SE, Mahnkopf M, Koch A, Tamura T: **Myc target gene, long intergenic noncoding RNA, Linc00176 in hepatocellular carcinoma regulates cell cycle and cell survival by titrating tumor suppressor microRNAs**. *Oncogene* 2018, **37**(1):75-85.
32. Rui X, Xu Y, Huang Y, Ji L, Jiang X: **lncRNA DLG1-AS1 Promotes Cell Proliferation by Competitively Binding with miR-107 and Up-Regulating ZHX1 Expression in Cervical Cancer**. *Cell Physiol Biochem* 2018, **49**(5):1792-1803.
33. Shen SN, Li K, Liu Y, Yang CL, He CY, Wang HR: **Silencing lncRNAs PVT1 Upregulates miR-145 and Confers Inhibitory Effects on Viability, Invasion, and Migration in EC**. *Mol Ther Nucleic Acids* 2020, **19**:668-682.

Figures

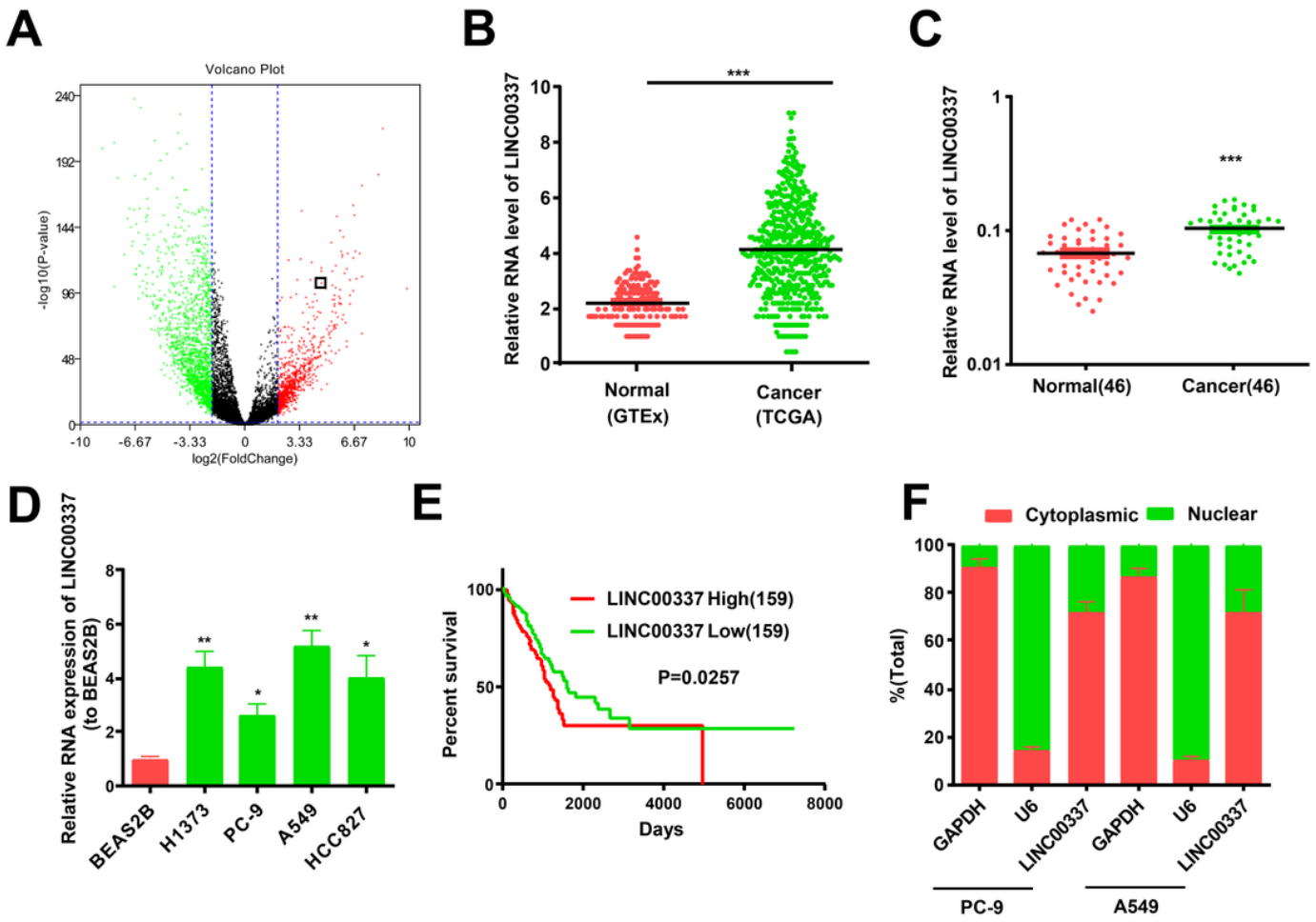

Figure 1

LINC00337 is raised in lung adenocarcinoma tissues and cells and mostly present in the cell cytoplasm (A) Volcano plot of TCGA + GTEx database, and LINC00337 is raised in lung adenocarcinoma. (B) The RNA level of LINC00337 in lung adenocarcinoma samples (from TCGA database) and normal samples (from GTEx database). (C) LINC00337 expression in 46 pairs of lung adenocarcinoma tissues and para-tumor tissues from our data. (D) LINC00337 expression in lung adenocarcinoma PC-9, H1373, HCC827 and A549 cell lines and normal human lung epithelial BEAS2B cell line. (E) Kaplan-Meier curves of overall survival from TCGA database. (F) Localization of LINC00337 by nucleocytoplasmic separation experiment. Data represent the mean ± SD; *P < 0.05, ** P < 0.01, ***P < 0.001.

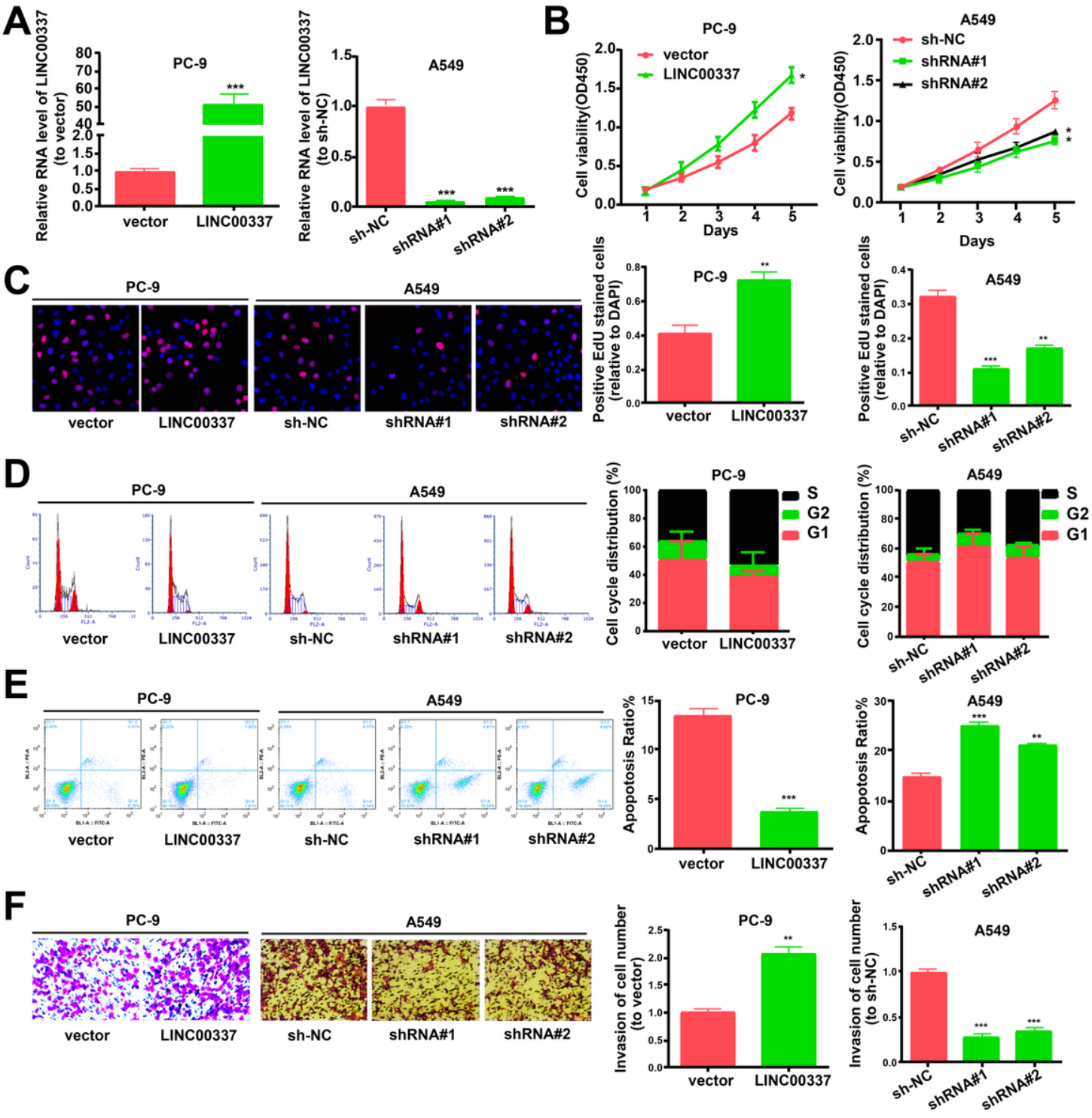

Figure 2

Knock-down of LINC00337 curbs proliferation, cycle and invasion, and boosts apoptosis of lung adenocarcinoma cells (A) Transfection efficiency of sh-LINC00337#1(shRNA#1), sh-LINC00337 #2(shRNA#2) and LINC00337-overexpressing vector (LINC00337). (B) CCK-8, and (C) EdU assay were performed to test cell proliferation. (D) The influence of LINC00337 on cell cycle. (E) The influence of LINC00337 on cell apoptosis. (F) Transwell assay ascertained cell invasion. Data were presented as represent the mean ± SD of 3 independent experiments; *P < 0.05, ** P < 0.01, ***P < 0.001.

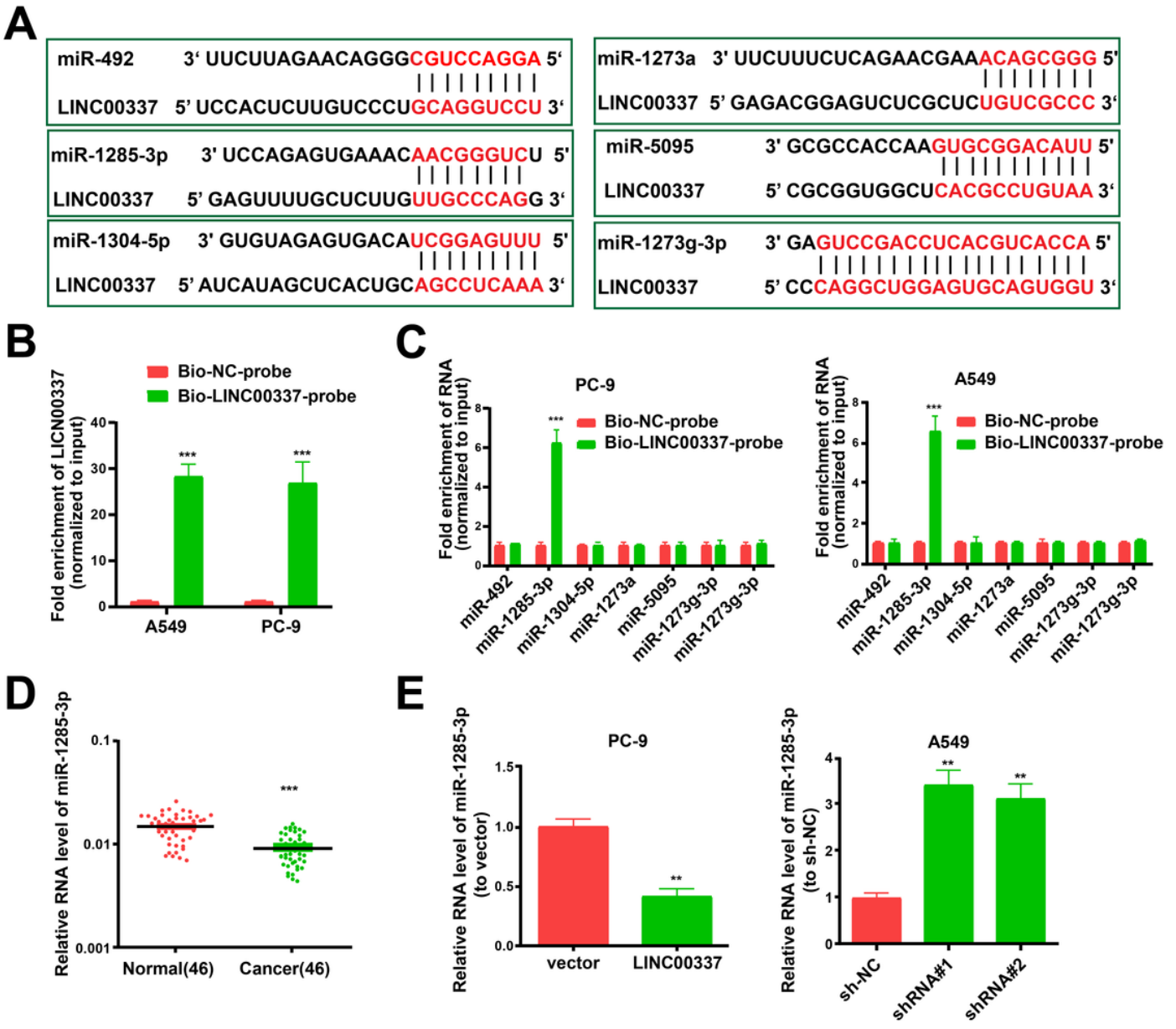

Figure 3

LINC00337 interplays with miR-1285-3p directly (A) Supposed binding sequence of LINC00337 with miR-1285-3p, miR-1304-5p, miR-492, miR-1273a, miR-5095, and miR-1273g-3p, as forecasted by RegRNA 2.0. (B) Detection of LINC00337 using qRT-PCR in the sample pulled down by biotinylated LINC00337 and negative control probe. (C) Examination of miR-492, miR-1285-3p, miR-1304-5p, miR-1273a, miR-5095, and miR-1273g-3p in the same sample reduced by biotinylate LINC00337 and NC probe. (D) The level of miR-1285-3p in 46 pairs of lung adenocarcinoma and para-tumor tissues. (E) The expression levels of miR-1285-3p in cells undergoing two shRNA or LINC00337 transfection were evaluated by qRT-PCR. Data represent the mean ± SD; ** P < 0.01, ***P < 0.001.

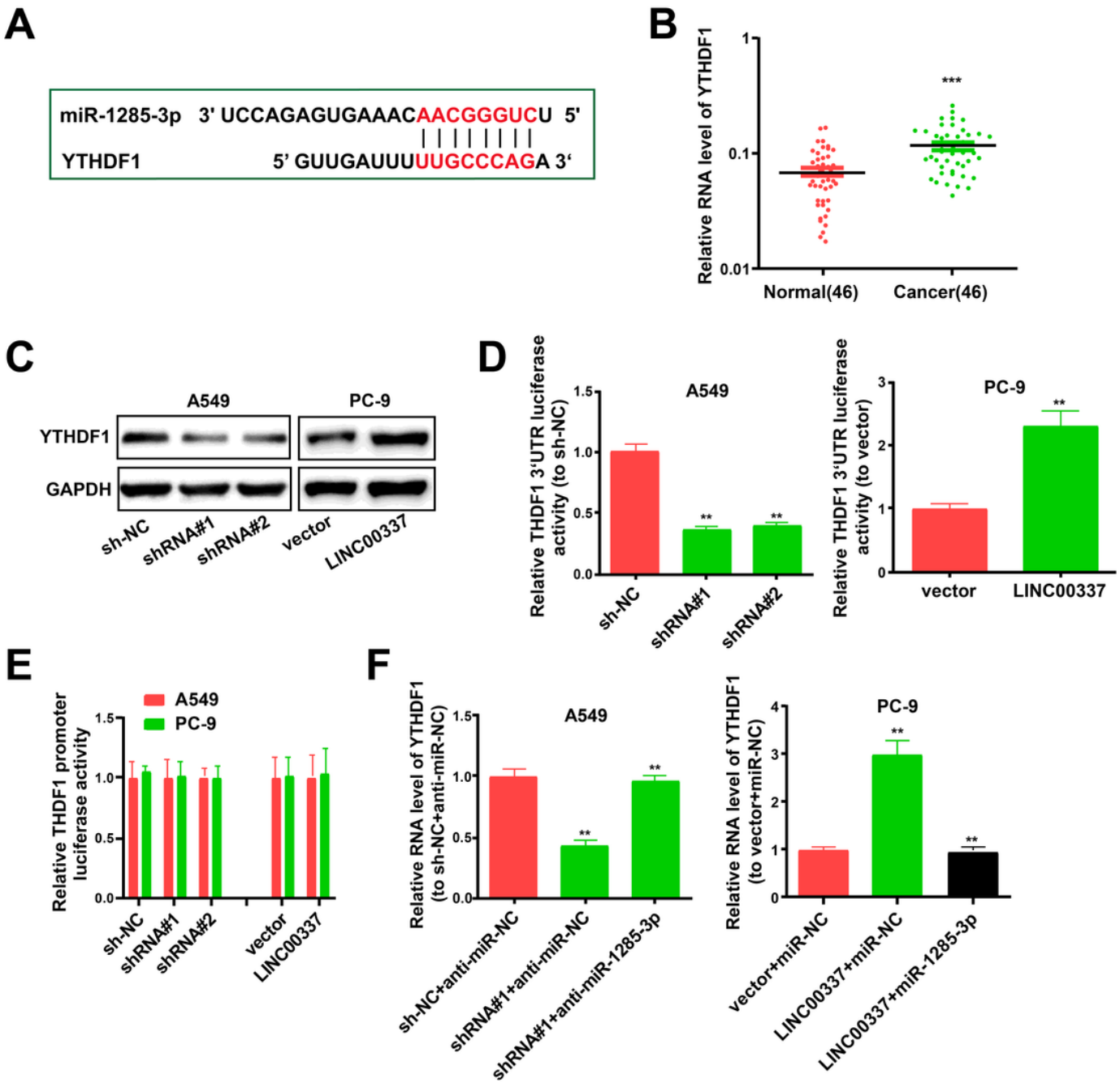

Figure 4

LINC00337 controls the miR-1285-3p target gene, YTHDF1 (A) Proposed binding sequence of miR-1285-3p with YTHDF1. (B) YTHDF1 level in 46 paired lung adenocarcinoma and para-tumor tissues. (C) The protein levels of YTHDF1 in cells undergoing shRNA or LINC00337 transfection were evaluated by western blot assay, with GAPDH as standard. (D) Relative luciferase activities of YTHDF1 3'-UTR reporter in stable A549 and PC-9 cells undergoing shRNA or LINC00337 transfection were examined using the Dual-Luciferase Reporter Assay System. (E) Relative luciferase activities of YTHDF1 promoter reporter in stable A549 and PC-9 cells receiving shRNA or LINC00337 transfection were detected. (F) YTHDF1

expression level in stable A549 and PC-9 cells after transfection. Data represent the mean ± SD; ** P < 0.01, ***P < 0.001.

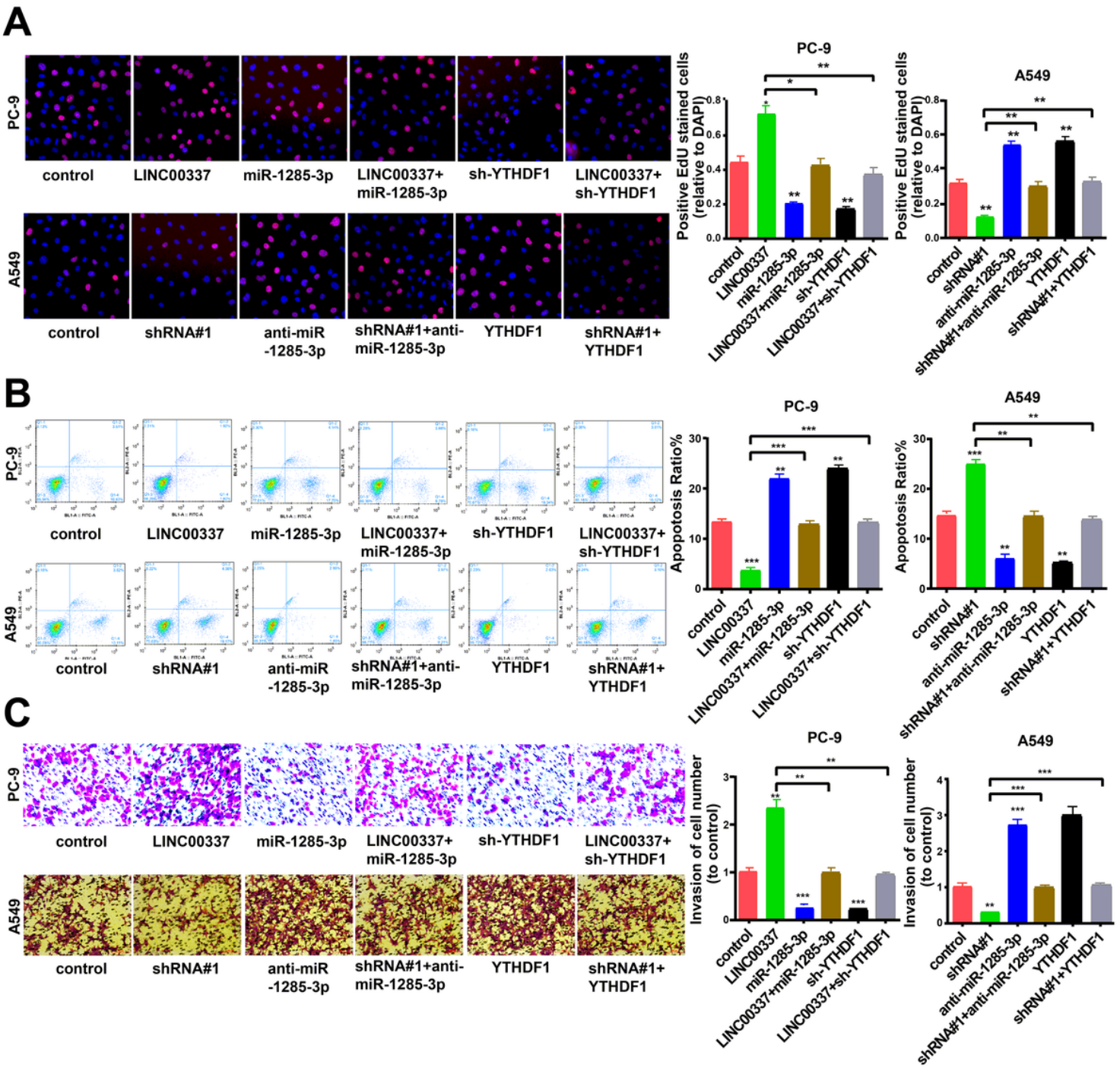

Figure 5

LINC00337/ miR-1285-3p / YTHDF1 axis controls behaviors of lung adenocarcinoma cells (A) Using EdU assay to detected A549 and PC-9 cell proliferation subsequent to transfection. (B) Apoptosis of A549 and PC-9 cells after transfection was detected. (C) A549 and PC-9 cell invasion subsequent to transfection was assessed. Data were presented as represent the mean ± SD of 3 respective experiments; *P < 0.05, ** P < 0.01, ***P < 0.001.

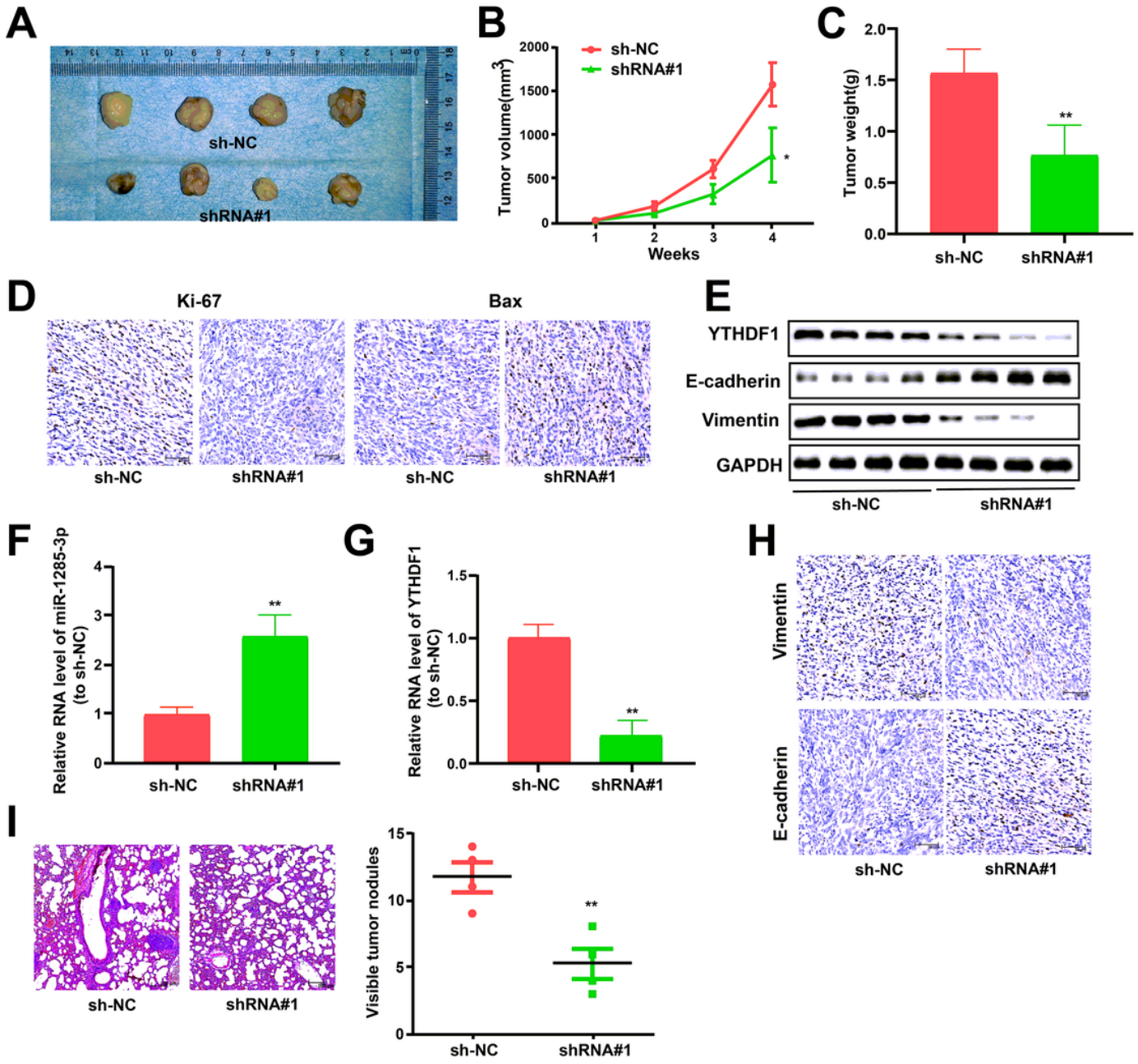

Figure 6

Inhibition of LINC00337 suppresses lung adenocarcinoma tumor to grow and metastasize in vivo (A) Images of xenografts. (B) Tumor volume and (C) weight data of orthotopic xenografts. (D) Ki-67 was used to assess proliferation via immunohistochemical staining, and Bax was utilized for apoptosis assay. (E) Western blot was used to assess the protein level of YTHDF1, E-cadherin, and Vimentin in tumors. (F) MiR-1285-3p and (G) YTHDF1 levels in tumors were detected. (H) Vimentin and E-cadherin from tumors were assessed via immunohistochemistry. (I) HE stained lung sections. Data represent the mean ± SD; *P < 0.05, ** P < 0.01.

Supplementary Files

This is a list of supplementary files associated with this preprint. Click to download.

- Additionalfile1.docx